Mixed-Mode Crack Tip Parameters Characterization from Image Correlation Technique

M. MEITE[a], O. POP[a], F. DUBOIS[a], J. ABSI[a]

a. *Group Studies of heterogeneous Materials, Civil Engineering and Durability, University of Limoges, 19300 Egletons, France*

Résumé :

Cet article traite de l'utilisation de la corrélation d'image numérique (DIC) pour séparer les facteurs d'intensité de contrainte (SIF), et les facteurs d'intensité d'ouverture de la fissure (SOIF) en mode mixte de rupture dans des milieux isotropes. Pour prédire ces paramètres de fissuration à partir de la technique de corrélation d'images, le développement asymptotique du champ de déplacement dans le voisinage de la pointe de fissure est employé. Une résolution non linéaire, par les moindres carrés, est mise en œuvre afin d'optimiser les champs expérimentaux par un des déplacements théoriques à partir duquel sont évaluées les propriétés de rupture en mode mixte.

Abstract :

This paper focuses on the application of the Digital Image Correlation (DIC) to properly separate the mixed-modes stress intensity factors (SIF) and crack opening intensity factors (SOIF) for cracks in isotropic media. To predict these crack tip parameters from DIC, the asymptotic expansion of the crack-tip displacement field is required. Over-deterministic nonlinear least-squares analyses of crack-tip displacements are used to obtain the best fit theoretical displacement field from which mixed-mode fracture properties are evaluated.

Keywords: Fracture Mechanics, Crack tip parameters, DIC, Nonlinear least-squares, Finite Element Method.

Introduction

Most structural components undergo complex loading in service conditions involving a combination of tension (mode I), in-plane shear (mode II) and often out-of-plane shear (mode III). A crack in such loading conditions is therefore likely to be subjected to mixed-mode loading at the crack tip. Thus, understanding the crack growth process under mixed-mode conditions in materials is an important aspect of structural integrity analysis. There is also a strong need to separate fracture modes for cracked specimens under ill-defined mixed mode loading. Several investigations have been developed to characterize crack tip parameters for fracture modes separation [10]. But, due to difficulty to assess these effective crack tip parameters, fascinating robust tools still need to be developed, taking into consideration current material mechanical properties, the kinetics of crack opening and the cracking properties.

This work aims to associate experimental full-fields information of Digital Image Correlation (DIC) to numerical Finite Element Modeling (FEM). The combined technique originates inverse method providing material mechanical properties used conveniently to characterize the mixed-mode energy release rate uncoupling.

In what follows, the theoretical formulation of mixed-mode crack tip parameter [3] is first provided and next; a brief description of the DIC method is outlined; and finally the experimental and numerical results are presented and discussed.

1 Linear Elastic Fracture Mechanics (LEFM)

1.1 Static approach

1.1.1 The MΘ-Integral concepts

The MΘ-integral is an energy parameter defined to analyze the crack growth in mixed-mode fracture by isolating different fracture modes, such as modes I and II parts, by means of a pseudo potential, combining the real, u_i, and auxiliary, v_i, fields through a generalization of the virtual work principle [3]:

$$M\theta = \frac{1}{2}\cdot\int_V \left(\sigma_{ij}^u \cdot v_{i,k} - \sigma_{ij,k}^v \cdot u_i\right)\cdot\theta_{k,j}\cdot dV \tag{1}$$

where path V is a ring bounded by two contours defined by a vector field $\vec{\theta}$. This vector $\vec{\theta}$ is continuously derivable and its components were defined as $\theta_1 = 1$ and $\theta_2 = 0$ inside the ring and then $\vec{\theta} = \vec{0}$ outside it [4].

1.1.2 Physical interpretation of the MΘ-Integral

When real, u_i, and auxiliary, v_i, cinematically admissible displacement fields are respectively identical, the following physical interpretation of MΘ-integral is available [4].

$$M\left(u,u\right) = J = G \tag{2}$$

where G defines energy release rate for the cracked specimen. Then, thanks to the superposition principle, one proposed the relation:

$$M\left(u,v\right) = C_\alpha \cdot \frac{{}^u K_\alpha^{(\sigma)} \cdot {}^v K_\alpha^{(\sigma)}}{8} \tag{3}$$

with, C_α is the reduced elastic compliance and α specifies the loading modes configuration such as I and II. Hence, choosing judicious values for the virtual stress intensity factor, ${}^v K_\alpha^{(\sigma)}$, the uncoupling fracture mode is obtained thru the real stress intensity factor, ${}^u K_\alpha^{(\sigma)}$ for the given mode $\alpha = I, II$ as follow:

$${}^u K_I^{(\sigma)} = \frac{8\cdot M\left(u,v\right)\cdot\left({}^v K_I^{(\sigma)} = 1, {}^v K_{II}^{(\sigma)} = 0\right)}{C_I} \quad \text{and} \quad {}^u K_{II}^{(\sigma)} = \frac{8\cdot M\left(u,v\right)\cdot\left({}^v K_I^{(\sigma)} = 0, {}^v K_{II}^{(\sigma)} = 1\right)}{C_{II}} \tag{4}$$

1.2 Kinematic approach: Crack Opening Intensity Factor concept

The concept of Crack Opening Intensity Factor, $K_\alpha^{(\varepsilon)}$ has been introduced to characterize the kinematic state of crack opening through displacements of two opposite points located on each crack lip [4]:

$$\left[u\right]_i = K_\alpha^{(\varepsilon)} \cdot \left(\frac{r}{2\cdot\pi}\right)^{0.5} \tag{5}$$

2 Experimental analysis by DIC

2.1 Experimental setup

The experimental procedure deals with specimen's surface displacement fields measurement by DIC, especially into crack tip domain. SEN (Single Edge Notch) specimens made of polymer (PVC) material are used for experimental test. These specimens are subjected to a tensile test in mixed-mode loading. The geometrical dimensions of these specimens are: *210x150x10mm*^{3} and the crack length is *70 mm*. A Zwick testing machine is used under displacement control with mobile cross-bare velocity of *0.1 mm/min*. Mixed-mode loading applied to cracked specimen is carried out by means of the Arcan Fixtures [9]. During this process, the crack, without propagating, was loaded elastically under several combinations of mixed-mode (I+II) displacements. So, both LVDT sensor and loading cell record the specimen behavior, while successive images of the sample surface before and after the deformation were recorded at each time step using a high resolution digital CCD camera. The CCD camera is rotated in order to appropriately measure the displacement fields in opening and in shear modes. Marks Tracking Method (MTM) was employed to

achieve synchronization process between testing machine data and recorded images (figure 1.a, b).

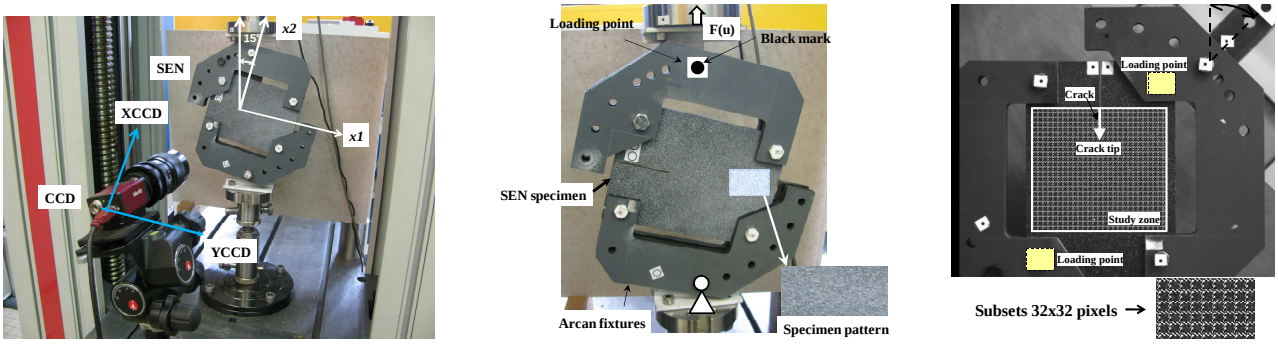

a. b. c.

FIG. 1 – Loading system and acquisition devices (a) and PVC SEN specimen with Arcan Fixtures (b).

2.2 Digital Image Correlation (DIC)

A digital image is essentially a two-dimensional array of intensity values which can be discretized into small subsets. Image correlation works by matching small square subsets of an undeformed image to locations in the image of the surface after deformation by means of a series of mathematical mapping and cross correlation functions [2]. For this technique to work well, a grey scale random pattern is needed on the surface of the specimen (figure.1.b). To recognize this pattern mathematically, the intensity of each pixel in the reference and deformed images can be traced and the displacement vector can be determined. Figure 1.c shows the arbitrary selected area subdivided into subsets of *32* by *32* pixels to make displacement fields analysis by Correla Software developed by Photomechanical and Rheology team of LMS Poitiers [1]. Because of experimental noises making the displacement data obtained from an experiment to include measurement error, it is very difficult to accurately analyze stress and strain fields from raw displacement data [7]. In addition, real deformation fields of the crack tip and its location, and the crack face are also difficult to be precisely obtained [10]. Consequently, optimization procedure is necessary to circumvent those difficulties.

3 Experimental fields optimization

Because crack tip parameters predicted from experimental raw displacement data are inaccurate, we proposed the solution which consists in substituting the measured field by a theoretical field whose parameters are optimized with respect to the experimental fields. Indeed, Kolossov-Muskhelishvili's mixed-mode analytical fields solution described in the mathematical series has been chosen to capture displacement fields of any point located near and far from the crack tip by developing series expansion [5, 10]:

$$u_1^k = \sum_{i=1}^{N}\left(A_I^i \cdot r_k^{(i/2)} \cdot f_i(\kappa,\theta_k) + A_{II}^i \cdot r_k^{(i/2)} \cdot g_i(\kappa,\theta_k) \right) + T_1 - R \cdot x_2^k$$

$$u_2^k = \sum_{i=1}^{N}\left(A_I^i \cdot r_k^{(i/2)} \cdot l_i(\kappa,\theta_k) + A_{II}^i \cdot r_k^{(i/2)} \cdot z_i(\kappa,\theta_k) \right) + T_2 + R \cdot x_1^k \qquad (6)$$

where N provides the number of terms in the series expansion of the displacement field, A_α^i are series coefficients when the loading mode is given by α = I, II. $f_i(\kappa,\theta)$, $g_i(\kappa,\theta)$, $l_i(\kappa,\theta)$ and $z_i(\kappa,\theta)$ are all polar functions defined by:

$$f_i(\kappa,\theta) = \kappa \cdot \cos\left(\frac{i}{2}\cdot\theta\right) - \frac{i}{2}\cdot\cos\left(\frac{i}{2}-2\right)\cdot\theta + \left\{\frac{i}{2}+(-1)^i\right\}\cdot\cos\left(\frac{i}{2}\cdot\theta\right)$$

$$g_i(\kappa,\theta) = -\kappa \cdot \sin\left(\frac{i}{2}\cdot\theta\right) + \frac{i}{2}\cdot\sin\left(\frac{i}{2}-2\right)\cdot\theta - \left\{\frac{i}{2}-(-1)^i\right\}\cdot\sin\left(\frac{i}{2}\cdot\theta\right)$$

$$l_i(\kappa,\theta)=\kappa\cdot sin\left(\frac{i}{2}\cdot\theta\right)+\frac{i}{2}\cdot sin\left(\frac{i}{2}-2\right)\cdot\theta-\left\{\frac{i}{2}+(-1)^i\right\}\cdot sin\left(\frac{i}{2}\cdot\theta\right)$$

$$z_i(\kappa,\theta)=+\kappa\cdot cos\left(\frac{i}{2}\cdot\theta\right)+\frac{i}{2}\cdot cos\left(\frac{i}{2}-2\right)\cdot\theta-\left\{\frac{i}{2}-(-1)^i\right\}\cdot cos\left(\frac{i}{2}\cdot\theta\right) \quad (7)$$

The subscript k in Eq. (6) denotes the index of the function evaluated at any point (r_k,θ_k), which corresponds to the displacement characterized by its components u_1^k and u_2^k:

$$r_k=\sqrt{\left(x_1^k-x_1^o\right)^2+\left(x_2^k-x_2^o\right)^2}\ ;\ \theta_k=\tan^{-1}\left(\frac{x_2^k-x_2^o}{x_1^k-x_1^o}\right)-\omega_o \quad (8)$$

where, x_1^o and x_2^o are the crack tip location relative to an arbitrary coordinate system and ω_o being an overall crack orientation. Coefficient κ is linked to material Poisson's ration ν, ($\kappa=(3-\nu)/(1+\nu)$ for plane stress), and rigid body motions such as translations in x_1-direction, x_2-direction and rotation are defined by the terms T_1, T_2 and R respectively. Thus, experimental field optimization is established by identifying different coefficients $A_I^1,\cdots,A_I^i$, $A_{II}^1,\cdots,A_{II}^i$, T_1, T_2 and R minimizing difference between measured field and analytical field through correlation algorithm in the least square sense:

$$\xi=\frac{\sum_{i=1}^{M}\left|U_{Th}^i-U_{Exp}^i\right|}{M} \quad (9)$$

where U_{Th}^i and U_{Exp}^i are respectively overall analytical and experimental fields while M corresponds to total number of measured data points.

Furthermore, since it is difficult to estimate accurately the crack tip position, the system of matrix (6) becomes nonlinear. An iterative procedure of the Newton-Raphson method [8, 10,] based on over-deterministic nonlinear least-squares is used to refine the precise values of the coefficients ($A_I^1,\cdots,A_I^i$, $A_{II}^1,\cdots,A_{II}^i$, T_1, T_2, R, x_1^0, x_2^0, κ et ω_0) minimizing error between asymptotic and measured fields.

4 Results and discussions

4.1 Crack Opening Intensity Factors (COIF) calculations from DIC

The asymptotic field (6) equivalent to the measured field in the zone of interest is obtained with a full number of the series $N=9$ for each mixity ratio (0°, 15° and 75°), corresponding respectively to minimized residual errors $\xi(0°)=0.34\%$, $\xi(15°)=0.31\%$, $\xi(75°)=0.15\%$ as illustrated in figure 2. Consequently, good agreement is obtained between experimental and analytical fields deformed shapes for each mixity ratio (0°, 15° and 75°) (figure 3).

In the following, optimized fields are used to analyze the fracture properties. Thus, when comparing equations (5) and (6), one demonstrates that the crack opening intensity factor, $K_\alpha^{(\varepsilon)}$ for fracture modes separation can be directly linked to the first terms of series for each displacement component of the optimized displacement fields, such as:

$$K_I^{(\varepsilon)}=2\cdot A_I^1\cdot\sqrt{2\cdot\pi}\cdot(\kappa+1)\ \text{and}\ K_{II}^{(\varepsilon)}=-2\cdot A_{II}^1\cdot\sqrt{2\cdot\pi}\cdot(\kappa+1) \quad (10)$$

Figure 4 shows the plot of COIF for modes I and II versus number of terms of the series expansion.

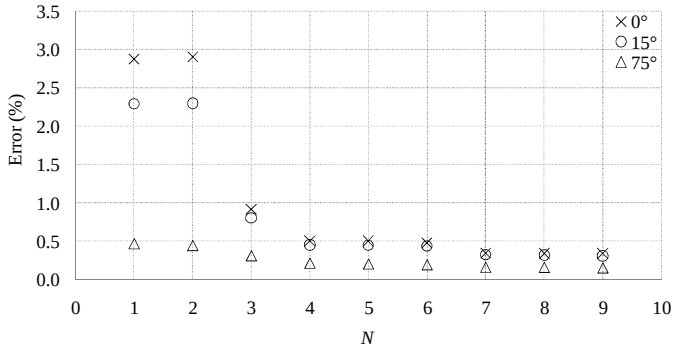

FIG. 2 – Error evolution versus number of terms into series (6)

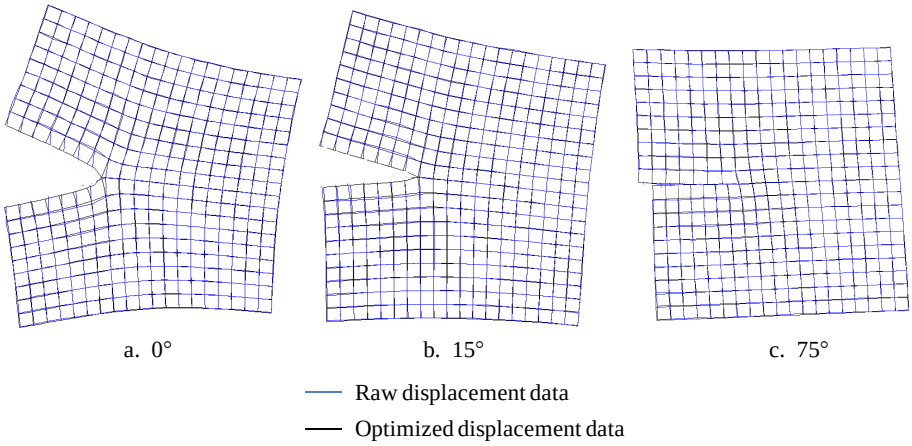

FIG. 3 – Deformed meshes of target area arbitrary selected into the crack tip vicinity.

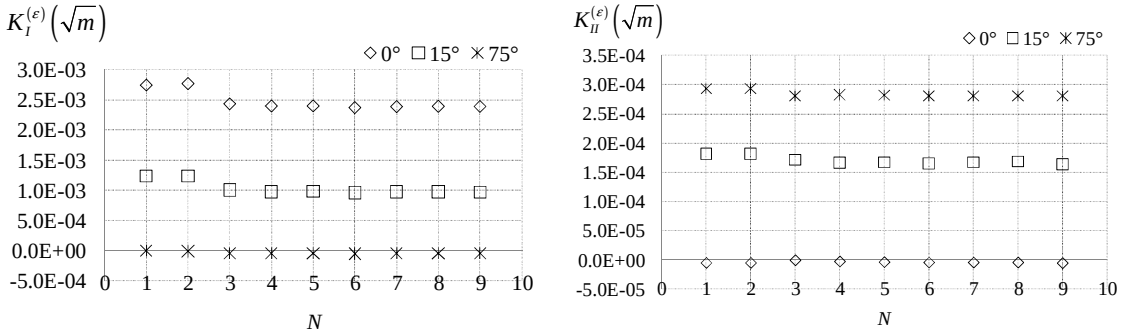

FIG. 4 – Crack Opening Intensity Factors versus number of series expansion.

4.2 Stress Intensity Factors (SIF) computation from FEM

Stress singularity into crack tip vicinity is characterized by SIF [6]. The amplitude of this crack tip singularity is not only proportional to the stress fields, the specimen geometry and its crack length, but not dependent on the material mechanical properties. So, finite element modeling of the experimental test with loading configuration is employed to compute real SIF, ${}^{u}K_{\alpha}^{(\sigma)}$, from (4). Note that, SIF calculation from FEM is curried out into the same integration domain like COIF of DIC; the target area being meshed with similar 4-nodes isoparametric elements. Loading values of *1515 N*, *1534 N* and *1261 N* are applied to the cracked specimen for each mixity ratio 0°, 15° and 75° respectively into complex loading area (figure 5).

Finally, combining COIF and SIF obtained respectively from DIC and FEM, the reduced elastic compliance, C_{α}, can be deduced, leading to the appropriate value identification of Young Modulus, E and the energy

release rate G_α ($\alpha = I, II$) for fracture modes uncoupling as:

$$E = 8 \cdot \frac{{}^{u}K_{\alpha}^{(\sigma)}}{K_{\alpha}^{(\varepsilon)}} \text{ and } G_\alpha = \frac{{}^{u}K_{\alpha}^{(\sigma)} \cdot K_{\alpha}^{(\varepsilon)}}{8} \tag{11}$$

According to (6) and (11), elastic properties obtained from the inverse method established in this work for PVC material, are approximately: $E = 2590MPa$, and $\nu = 0.379$. The values of the mixed-mode energy release rate for fracture modes separation are given in the table 1 bellow:

Table 1: Mixed-mode energy release rate uncoupling for different mixity ratio 0°, 15° and 75°.

	0°	15°	75°
$G_I \left(J \cdot m^{-2} \right)$	231.64	37.72	≈ 0
$G_{II} \left(J \cdot m^{-2} \right)$	≈ 0	1.05	3.18

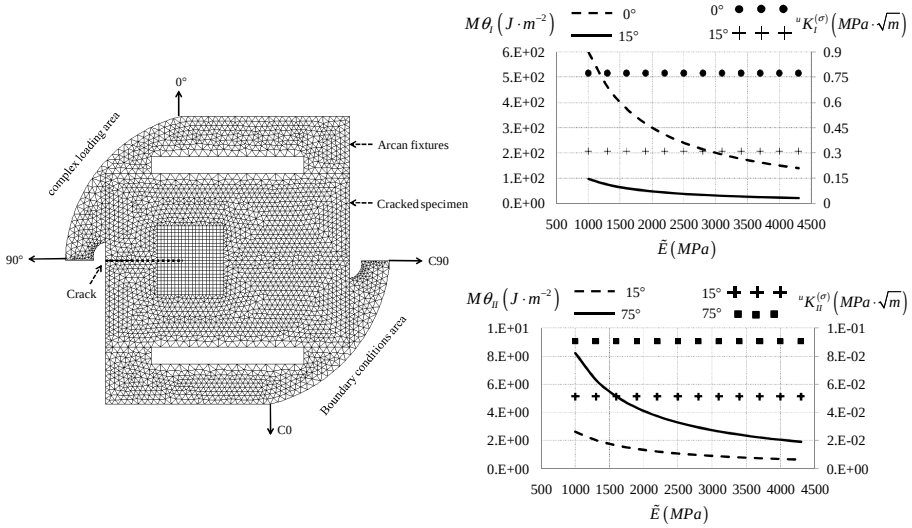

FIG. 5 – Finite elements modeling and crack tip parameters evolution versus Young modulus.

Conclusions and perspectives

The present investigation is viewed as a main contribution to properly separate fracture modes in mixed-mode loading through the hybrid experimental and numerical approaches. Experimental full-fields information provided by DIC, after optimization by means of over-deterministic nonlinear least-squares, is used to determine the Crack Opening Intensity Factors (COIF) in modes I and II. Moreover, finite element modeling of such experimental test, in complex loading configuration, yields the Stress Intensity Factors (SIF) computation for both modes I and II separately via $M\theta$-integral concept. The combination of COIF and SIF results in current material mechanical properties identification necessarily used to accurately characterize the energy release rate for mixed-mode fracture uncoupling.

As fracture modes separation is successfully characterized through this work, an extension of the developed algorithm can be established for orthotropic media under mixed-mode loading configuration.

References

[1] Bretagne N., Valle V., Dupre J.C.: Development of the marks tracking technique for strain field and volume variation measurements, NDT&E International, 38, 290–298, 2005.
[2] Clocksin W.F., Quinta da Fonseca J., Withers P.J., Torr P.H.S., Image processing issues in digital strain mapping, Proc SPIE 4790:384–395, 2002.

[3] Chen F. H. K., Shield R. T., Conservation laws in elasticity of the J-integral type. Journal of Applied Mechanics and Physics 28 1–22, 1977.
[4] Dubois F., Modélisation du comportement mécanique des milieux viscoélastiques fissurés: Application au matériau bois, Thèse de doctorat de l'Université de Limoges, 1997.
[5] Hamam R., Hild F. Roux S., Stress Intensity Factor Gauging by Digital Image Correlation: Application in Cyclic Fatigue, *Strain* 43, 181–192, 2007.
[6] Irwin G.R. « Analysis of stresses and strains near the end of crack traversing a plate », Journal of Applied Mechanics, 24, 1957, 361-364B., Frame uncoupling, Rapt Journal, 1, 21-32, 1982
[7] Kenji M., Yoshimasa S., Examination of the accuracy of the singular Stress Field Near a Crack-tip by Digital Image Correlation, Key Engineering Material Vols. 321-323, pp. 32-37, 2006.
[8] Sanford, R. J., Application of the least-squares method to photoelastic analysis. Exp. Mech. 20, 192–197, 1980.
[9] Yen S.-C., Craddock J.N., Teh K.T., Evaluation of a modified arcan fixture for the in-plane shear test of materials, Experimental Techniques, 12(12), 22-25, 2008.
[10] Yoneyama S., Morimoto Y. and Takashi M., Automatic Evaluation of mixed-mode stress intensity factors utilizing digital image correlation, Strain, 42, 21-29, 2006.